

Newfoundland and Labrador Hydro Hydro Place. 500 Columbus Drive P.O. Box 12400. St. John's. NL Canada A1B 4K7 t. 709.737.1400 I f. 709.737.1800 nlhydro.com

October 16, 2025

Board of Commissioners of Public Utilities Prince Charles Building 120 Torbay Road, P.O. Box 21040 St. John's, NL A1A 5B2

Attention: Jo-Anne Galarneau

Executive Director and Board Secretary

Re: Application for Capital Expenditures for the Life Extension of Bay d'Espoir Unit 7 – Request for Additional Information – Hydro's Reply

Newfoundland and Labrador Hydro ("Hydro") filed its application for approval of the capital expenditures required for the life extension of Unit 7 of the Bay d'Espoir Hydroelectric Generating Facility ("Bay d'Espoir Unit 7") on June 20, 2025 ("Life Extension Application").

On August 8, 2025, the Board of Commissioners of Public Utilities ("Board") requested analysis of an additional alternative to address the life extension of Bay d'Espoir Unit 7, specifically the uprate of the unit. Hydro filed its response to the Board's request for additional information on September 22, 2025¹ ("Hydro's Reply"), in which Hydro concluded that the planned life extension of Unit 7, along with the installation of Unit 8 proposed in Hydro's 2025 Build Application,² represents the most optimal solution for the Island Interconnected System.

On October 6, 2025, the Board requested additional information relating to conclusions made in a report provided as Attachment 2 to Hydro's Reply,³ specifically, the issues of tailwater elevation restrictions and Unit 7's floating rim design. The requested information is provided herein.

Tailwater Elevation Restrictions

As noted in the GE Hydro Report, tailwater elevation was identified as a limiting factor for the practical uprating of Bay d'Espoir Unit 7, as higher turbine outputs were contingent on the availability of elevated tailwater levels to provide adequate cavitation protection. The report concluded that, based on the observed tailwater elevations at that time, the useful capacity increase would be limited to approximately 5 MW.

The Uprate Report,⁴ prepared by Hatch Ltd. ("Hatch") in 2024, noted that tailrace elevation data collected between 2010 and 2018 varied from those referenced in the 2004 GE Hydro Report; the data

¹ "Bay d'Espoir Unit 7 Additional Analysis Report," Newfoundland and Labrador Hydro, rev. September 23, 2025 (originally filed September 22, 2025).

² "2025 Build Application – Bay d'Espoir Unit 8 and Avalon Combustion Turbine," Newfoundland and Labrador Hydro, March 21, 2025.

³ "Bay d'Espoir Generating Station Unit 7 Runner Replacement," Generation Engineering, April 6, 2004 ("GE Hydro Report").

⁴ "Uprate Report," Hatch Ltd, June 27, 2024, provided in "2024 Resource Adequacy Plan – An Update to the Reliability and Resource Adequacy Study," Newfoundland and Labrador Hydro, rev. August 26, 2024 (originally filed July 9, 2024), app. C, att. 2.

generally ranged between 1.0 and 2.8 metres with an average of approximately 2.0 metres. Hatch concluded that turbine operation up to 180 MW should be feasible within this range.

Hydro confirms that considerations regarding tailwater elevation remain valid from a technical perspective and would require detailed feasibility assessment and engineering analysis to quantify their present-day impacts. Tailrace elevations will also be influenced by the addition of Bay d'Espoir Unit 8, which will alter the system's hydraulic regime. As such, the potential impacts of tailwater elevation on any future uprating of Unit 7 would need to be evaluated within the context of the overall Bay d'Espoir system, including the planned Unit 8 addition.

Hydro has not undertaken this additional feasibility assessment, as Hydro's basis for not pursuing uprating of Unit 7 are the hydrologic, efficiency, cost, and schedule factors outlined in Hydro's Reply. Hydro's opinion is that those factors eliminate the uprating of Unit 7 as an appropriate alternative, regardless of the tailwater elevation issues.

Floating Rim Design

Bay d'Espoir Unit 7 is equipped with a floating rim generator rotor design. This design, which was used by General Electric in the 1970s, often had balance problems associated with overspeed events. The rotor rim components would move slightly during an overspeed, necessitating rebalancing after the unit trip. In the 1990s, Hydro completed the installation of additional rim guide blocks on the rotor spider, a mitigation to resist the movement of the rim; however, the work did not completely eliminate the issue. In the early 2000s, Hydro undertook engineering assessments to further address the vibration and balance concerns, including the Rotor Rim Shrink Study completed by GE Hydro in 2000, provided as Attachment 1 hereto. That study evaluated the feasibility of stiffening the rotor spider to permit a higher rim shrink to increase the force holding the rim in position.

While the solution noted above was not implemented, Hydro completed maintenance intervention and balancing activities in the mid-2010s and has subsequently seen improvement in the post-overspeed performance of the floating rim. The unit has experienced three overspeed events following load rejections in the last ten years. The latest two trips in 2017 and 2022 did not require rebalancing. Despite this performance improvement, the concerns regarding the floating rim design are still valid, as more frequent or longer duration overspeed events have the potential to result in similar balance issues.

The 2004 GE Hydro Report uprate proposals⁵ included an estimate for a replacement spider designed to transmit the increased power generated by the uprated runner, and with a modern key system to maintain the balance during overspeed.

Hydro does not plan to replace the spider as part of the life extension project. To monitor the condition of the floating rim design, Hydro regularly completes visual inspections of the rotor to monitor for signs of excessive movement, such as fretting or cracking in the guide block and keying system. No concerns have been identified from these inspections. A more detailed inspection, including non-destructive examination of all rotor rim guidance blocks and key assemblies, is planned as part of the 2026 PM9 scope.

While both the tailwater elevation constraints and the floating rim generator design present significant technical complexities that would require extensive feasibility studies, engineering assessment and design, and potential component modifications, Hydro believes that incurring the additional substantial

⁵ Supra, f.n. 3, att. 2, app. II.

time and cost to address these issues is not a necessary, prudent, or cost-effective approach. Hydro's analysis has concluded that proceeding with the planned life extension, in conjunction with the installation of Unit 8, is the most optimal solution for the Island Interconnected System, ensuring cost efficiency, reliability, and hydrological sustainability.

Should you have any questions or comments, please contact the undersigned.

Yours truly,

NEWFOUNDLAND AND LABRADOR HYDRO

Shirley A. Walsh

Senior Legal Counsel, Regulatory SAW/kd

Encl.

ecc:

Board of Commissioners of Public Utilities

Jacqui H. Glynn Ryan Oake Board General

Island Industrial Customer Group

Paul L. Coxworthy, Stewart McKelvey Denis J. Fleming, Cox & Palmer Glen G. Seaborn, Poole Althouse **Labrador Interconnected Group**

Senwung F. Luk, Olthuis Kleer Townshend LLP Nicholas E. Kennedy, Olthuis Kleer Townshend LLP

Consumer Advocate

Dennis M. Browne, KC, Browne Fitzgerald Morgan & Avis Stephen F. Fitzgerald, KC, Browne Fitzgerald Morgan & Avis Sarah G. Fitzgerald, Browne Fitzgerald Morgan & Avis Bernice Bailey, Browne Fitzgerald Morgan & Avis **Newfoundland Power Inc.**

Dominic J. Foley Douglas W. Wright Regulatory Email

Attachment 1, Page 1 of 34

BAY D'ESPOIR POWERSTATION UNIT 7 GENERATOR ROTOR RIM SHRINK STUDY

SEPTEMBER 2000

Completed by: Mike White

Wayne Martin

GE Hydro, Peterborough

TABLE OF CONTENTS

| Need for Rim Shrink on Bay D'Espoir Unit #7 | 1 |
|---|----------|
| 2. Level of Rim Shrink Required | 3 |
| 3. Radial Stiffness of Rotor Rim | 5 |
| 4. Shrink Temperature Difference for Rim | 10 |
| 5.1. Geometry of Combined Rotor Spider and Rim Model | 11 |
| 6.1. Standstill Buckling Analysis of Existing Rotor Spider | 13 14 |
| 7. Final Rotor Spider Dimensions | 16 |
| 8. Structural Analysis of Spider at Standstill Due to Shr 8.1. Deflection of Rotor Spider at Standstill Due to Shrink 8.2. Stress in Rotor Spider at Standstill Due to Shrink 8.3. Radial Force on Rotor Spider at Standstill Due to Shrink | 18 19 |
| 9. Recommendations for Rim Shrink | 23 |
| 10. Rim Shrink Procedure | 23 |
| 11. Rim Heaters | 29 |
| 12. Shrink Keys and Anti-buckling Stiffeners | 29 |

LIST OF FIGURES

| FIGURE 1: | RIM STIFFNESS FINITE ELEMENT RESULTS | 9 |
|-----------|--|----|
| FIGURE 2: | FINITE ELEMENT RESULTS FOR RIM 42.6°C COOLER THAN SPIDER | 11 |
| FIGURE 3: | ROTOR SPIDER AND RIM FINITE ELEMENT MODEL | 12 |
| FIGURE 4: | BUCKLING ANALYSIS OF EXISTING ROTOR SPIDER AT STANDSTILL | 14 |
| FIGURE 5: | ROTOR SPIDER AND RIM FINITE ELEMENT MODEL WITH SHRINK ANGLES | 15 |
| FIGURE 6: | BUCKLING ANALYSIS OF MODIFIED ROTOR SPIDER AT STANDSTILL | 16 |
| FIGURE 7: | CROSS KEY AND ANGLE SUPPORT DIMENSIONS | 17 |
| FIGURE 8: | DEFLECTION OF SPIDER AT STANDSTILL DUE TO SHRINK | 18 |
| FIGURE 9: | RADIAL DEFLECTION OF SPIDER AT STANDSTILL DUE TO SHRINK | 19 |
| FIGURE 10 | : VON MISES STRESS UP TO 36,000 [PSI] IN ROTOR SPIDER | 21 |
| FIGURE 11 | : VON MISES STRESS UP TO 68,000 [PSI] IN ROTOR SPIDER | 22 |
| FIGURE 12 | : ROTOR POSITION AND KEY MOVEMENTS | 27 |
| FIGURE 13 | : TYPICAL HEAT SHRINK KEY ARRANGEMENT | 28 |

1. Need for Rim Shrink on Bay D'Espoir Unit #7

Current the rotor on Bay D'Espoir unit #7 generator is a floating rim design, where the connection between the rim and rotor spider is provided by torque and guidance block and key assemblies. This system of keying has lead to problems with maintaining rotor balance on this hydroelectric generator. As a result, it is desired to shrink the rim onto the rotor spider to better maintain rotor balance. The purpose of this study is to investigate the feasibility of performing rim shrink on this spider, and to indicate changes to the rotor spider that will permit the rim to be shrink.

2. Level of Rim Shrink Required

There are two distinct reasons for shrinking the rim onto the rotor spider in vertical The first of these, usually of prime concern on larger axis hydrogenerators. diameter units, is to stabilise and control the rotor rim shape. During operation of the unit with the rotor poles energised (stator at rated voltage), the magnetisation of the poles and stator core creates a force condition in the air gap that, if unstable, attempts to make the rotor rim become out of round, usually into an oval shape. If the inherent mechanical ovalizing stiffness of the rim is greater than the destabilising air gap magnetic stiffness, then rim shrink is not needed to ensure rotor shape control. In the case where the mechanical stiffness is less than the air gap stiffness, supplemental radial support stiffness must be added to the rim stiffness. The objective of the rim shrink onto the rotor spider is to add the natural radial stiffness of the rotor spider to that of the rim, thereby creating an adequately stable rim / rotor structure. For the rotor spider to add its stiffness to the rim, it must be in contact with the rim. Therefore, the minimum required rim shrink interference is equal to the differential centrifugal expansion of the rim / poles from zero to the required shrink speed (to that of the rotor spider). Since the magnetic air gap load has a long-term presence only at rated speed, the rim shrink is only required to rated speed, to ensure proper rim shape control. It is prudent to initially shrink the rim to some speed higher than rated, to account for expected shrink reduction with time due to rim plate slip and material creep in the areas of shrink key high contact stresses. In practice, where shrink is required, the rims are initially shrunk to approximately 1.25 - 1.30 times rated speed. (Attempting to apply a rim shrink to higher separation speed does not add to the operating stability of the unit and would require significantly more robust and heavy rotor spiders to accept the very high shrink stresses.) For the Bay D'Espoir Unit 7 generator, the non-shrunk mechanical stiffness of the rotor rim is much greater than the air gap magnetic stiffness. Therefore, to maintain rim roundness stability, a shrunk rim is not necessary. That is, the rim will not collapse, or develop undue ovality, if a rim shrink is not in effect.

The second purpose for a shrunk rim is to help prevent the rim from developing excessive eccentricity, with respect to the rotor spider. This is especially significant in designs where the rim to spider keying system is marginal in its ability to create

adequate tangential stiffies to contain the rim concentric to the shaft. To create this function is the purpose of the rim shrink on the Bay D'Espoir 7 generator.

As indicated above, the present thinking within the industry is to shrink new generator rims, where rim ovality development is probable, to approximately 1.3 times rated speed. For the purpose of keeping the rim concentric to the shaft, there is an obvious need to do so up to full runaway speed. However, on almost all generators, shrinking to full runaway speed is not possible and the 1.3 times rated speed shrink level is viewed as the limit, even for units where shrink is necessary for rim concentric control. As such, for speeds exceeding the rim shrink separation speed, there is a need for other means of supplementary rim centering.

For the Bay D'Espoir 7 generator, an analysis was performed on the rotor to assess its capability to accept a shrink to 130% speed. The conclusion was that at the interference requirement for a 1.3 per unit speed shrink, the stresses induced in the existing rotor spider would be excessive. As well, the inward radial displacement of the rotor spider inner lower disk would be to an extent that the rotor spider to shaft coupling bolts would be shear bound to the point that the bolts could not be removed without removing the rim shrink. GE believes that this condition is unacceptable. To overcome this condition, a reduced level of shrink was evaluated. Since the existing generator has been in service for over 20 years, the rim has been expanded and "seasoned" to the point where future irreversible rim plate slippage is highly unlikely. As such, a part of the need to have an above rated speed shrink, as recommended for a new generator, does not apply to this unit. As well, this unit has been designed with a set of rim torque blocks and retrofitted with a rim upper guidance key block system, which will provide the needed position control of the rim for short-time, higher speed excursions.

Taking the above into account, GE has deemed that a rim shrink in the range of 1.10 to 1.15 per unit speed is sufficient to add a significant supplementary stiffness to the rim to shaft connection. With this conclusion, an analysis using a rim shrink interference equivalent to 1.15 per unit speed rim expansion, was completed and the results presented here.

C spiden

Our problem our folling ful low regition (1)

2.1. Radial Interference Between Rim and Spider Due to Shrink

Set Ibm to Represent Pounds Mass

1bm := 1b

Rim Dimensions

D_{orim}:=258.742in

Rim Outer Diameter

DEPTH rimgross := 21.000 in

Average Gross Rim Depth

DEPTH rimnet := 18.344 in

Average Net Rim Depth

HT rimpiled := 77.5 in

Axial Height of Piled Rim

Rotational Speed Information

RPM rated $= 225.0 \frac{1}{\text{min}}$

Rotational Speed at Rated Conditions

RPM runaway := 380.0 $\frac{1}{\text{min}}$

Rotational Speed at Runaway Conditions

FACT shrink := 1.15

Fraction of Rated Speed to Which Rim and Spider Remain in Contact Due to

Rim Shrink

Pole Information

F PerPoleRunaway := 28767471bf

Centripetal Force Per Pole at Runaway

Speed

N poles := 32

Number of Poles

Properties of Steel

 $\rho_{\text{steel}} := 0.283 \cdot \frac{\text{lbm}}{\text{in}^3}$

Density of Steel

 $E_{\text{steel}} := 30 \cdot 10^6 \cdot \frac{\text{lbf}}{\text{in}^2}$

Young's Modulus for Steel

Determine inside and outside radius of rim.

$$R_{\text{orim}} := \frac{D_{\text{orim}}}{2}$$

Rotational speed at which rim and spider lose contact.

RPM shrink := FACT shrink · RPM rated RPM shrink =
$$258.75 - \frac{1}{\text{min}}$$

$$ω$$
 shrink := RPM shrink $\cdot \left[\frac{2 \cdot \pi \cdot \text{rad}}{60 \cdot \left(\frac{\text{sec}}{\text{min}} \right)} \right]$ $ω$ shrink = 27.096 $\frac{1}{\text{sec}}$

shrink =
$$27.096 \frac{1}{\text{sec}}$$

Centripetal force per pole at shrink speed.

$$F_{PerPoleShrink} := F_{PerPoleRunaway} \cdot \left(\frac{RPM_{shrink}}{RPM_{runaway}} \right)^{2}$$

Centripetal force of all the poles at shrink speed.

F PolesShrink := F PerPoleShrink
$$\cdot$$
 N poles

Mass of the rim.

Mass
$$_{rim}$$
:= ρ $_{steel} \cdot \pi \cdot \left(R_{orim}^2 - R_{irim}^2\right) \cdot HT_{rimpiled}$

Mass
$$_{rim}$$
 = 3.44·10⁵ olbm

Radius to the centre of gravity of the rim.

$$R_{cgrim} := \frac{2}{3} \cdot \left| \frac{R_{orim}^{3} - R_{irim}^{3}}{R_{orim}^{2} - R_{irim}^{2}} \right|$$

Centripetal force of the rim at shrink speed.

$$F_{RimShrink} = Mass_{rim} (\omega_{shrink})^2 \cdot R_{cgrim}$$

Tangential force that occurs in rim due to centripetal force of the rim and poles.

$$F_{RimTension} := \frac{F_{RimShrink} + F_{PolesShrink}}{2 \cdot \pi}$$

$$F_{RimTension} = 1.92 \cdot 10^{7} \text{ olbf}$$

Average tangential stress in the rim at shrink speed due to the centripetal force of the rim and poles. This calculation assumes the stress is constant across the radial depth of the rim (i.e. thin ring theory). Note that the net rim depth is used in this calculation in order to account for the rim stud holes, and the pole dovetail slots in the rim.

A rim:= HT rimpiled DEPTH rimnet

A rim=
$$1.422 \cdot 10^3 \cdot \text{ein}^2$$

$$\sigma_{\text{rim}} := \frac{\text{F RimTension}}{\text{A rim}}$$

$$\sigma_{\text{rim}} = 1.351 \cdot 10^4 \cdot \frac{\text{lbf}}{\text{in}^2}$$

Radial growth of the rim from rest to shrink speed.

$$\epsilon_{\text{rim}} := \frac{\sigma_{\text{rim}}}{E_{\text{steel}}}$$

$$\epsilon_{\text{rim}} = 4.502 \cdot 10^{-4}$$

$$\Delta R_{\text{rimshrink}} := R_{\text{cgrim}} \cdot \epsilon_{\text{rim}}$$

$$\Delta R_{\text{rimshrink}} = 0.054 \cdot \epsilon_{\text{in}}$$

If the radial growth of the rotor spider from rest to shrink speed is neglected, then the interference between the rim and spider at standstill is equal to the radial growth of the rim. Therefore, the required radial interference between the rim and spider for shrink up to 115% of rated speed is 0.054 [in].

3. Radial Stiffness of Rotor Rim

The radial stiffness of the rotor rim is calculated as the stiffness of a cylinder to which evenly spaced radial loads are applied. All formulas for this calculation are given in Roark's Formulas for Stress & Strain (6th Edition) by Warren C. Young. A reduction factor is applied to the cross-sectional area of the rim to account for its segmental nature. Also, the assumption is made that the radial depth of material from the inner edge of the pole dovetails outward is not capable of supporting a tangential load. Therefore, the average net rim depth is used to determine the outer radius of the rim for the purpose of calculating rim stiffness.

Rim Dimensions

Rim Outer Diameter

Average Gross Rim Depth

Average Net Rim Depth

Axial Height of Piled Rim

Number of Poles per Rim Plate

Spider Dimensions

Number of Arms on the Rotor Spider.

Properties of Steel

$$E_{steel} := 29 \cdot 10^6 \cdot \frac{lbf}{in^2}$$

Young's Modulus for Steel

$$G_{steel} := 12.5 \cdot 10^6 \cdot \frac{lbf}{in^2}$$

Shear Modulus for Steel

Determine inside and outside radius of rim.

$$R_{\text{orim}} := \frac{D_{\text{orim}}}{2}$$

$$R_{irim}$$
:= R_{orim} - DEPTH rimgross

Effective outside radius of rim for hoop stress calculation.

One-half of the angle between rotor spider arms (page 268 of Roark).

$$\theta := \frac{2 \cdot \pi}{2 \cdot N \text{ SpidArms}}$$

$$\theta=0.393$$

Cross-sectional area of the rim. Note that FACTarea is used to accoun for the segmental nature of the rim.

FACT area :=
$$\frac{N \text{ PolesPerPlate} - 1}{N \text{ PolesPerPlate}}$$
 FACT area = 0.75

A :=
$$(R_{orimeff} - R_{irim}) \cdot HT_{rimpiled} \cdot FACT_{area}$$
 A = 1.06610³ oin²

Shear shape factor (page 201 Roark).

$$F := \frac{5}{6}$$

Inertia of rim cross-section.

$$I := \frac{1}{12} \cdot HT_{rimpiled} \left(R_{orimeff} - R_{irim} \right)^{3}$$

$$I = 3.987 \cdot 10^{4} \circ in^{4}$$

Average radius of rim.

$$R := \frac{R \text{ orimeff} + R \text{ irim}}{2}$$

$$R = 117.543 \text{ in}$$

Hoop-stress deformation factor (page 262 of Roark).

$$\alpha := \frac{I}{A \cdot R^2} \qquad \qquad \alpha = 2.706 \cdot 10^{-3}$$

Transverse (radial) shear deformation factor (page 262 of Roark).

$$\beta := \frac{\text{F} \cdot \text{E}_{\text{steel}} \cdot \text{I}}{\text{G}_{\text{steel}} \cdot \text{A} \cdot \text{R}^2}$$

$$\beta = 5.232 \cdot 10^{-3}$$

k constants (page 262 of Roark).

$$k_1 := 1 - \alpha + \beta$$
 $k_1 = 1.003$ $k_2 := 1 - \alpha$ $k_2 = 0.997$

s and c constants (page 262 of Roark).

 $c := cos(\theta)$

$$s := \sin(\theta) \qquad \qquad s = 0.383$$

$$k := \frac{E_{\text{steel}} \cdot I}{R^{3}} \cdot \frac{1}{\left[\frac{k_{1} \cdot (\theta - s \cdot c)}{4 \cdot s^{2}} + \frac{k_{2} \cdot c}{2 \cdot s} - \frac{k_{2}^{2}}{2 \cdot \theta}\right]}$$
 $k = 1.59 \cdot 10^{8} \circ \frac{\text{lbf}}{\text{in}}$

Stifffness of rim at each arm on the rotor spider (page 268 of Roark).

Therefore, the stiffness of the rim at each rotor spider arm is 1.59×10^8 [lbf/in]. This means that a radial force of 10×10^6 [lbf] applied to the inner edge of the rim should produce a radial deflection of 0.0629 [in].

c = 0.924

A finite element model representing the three rim-donuts on this machine was created to simulate the rim during shrinking. It was found, through a process of trial-and-error, that a rim stiffness of 1.59×10^8 [lbf/in] corresponds to a disc with a 216.7 [in] inside diameter and a 250.3 [in] outside diameter.

In order to verify that the rim has the required stiffness, a radial load of $10x10^6$ [lbf] was applied to the inner edge of the rim discs. The results from this finite element analysis are shown in **Figure 1: Rim Stiffness Finite Element Results.**

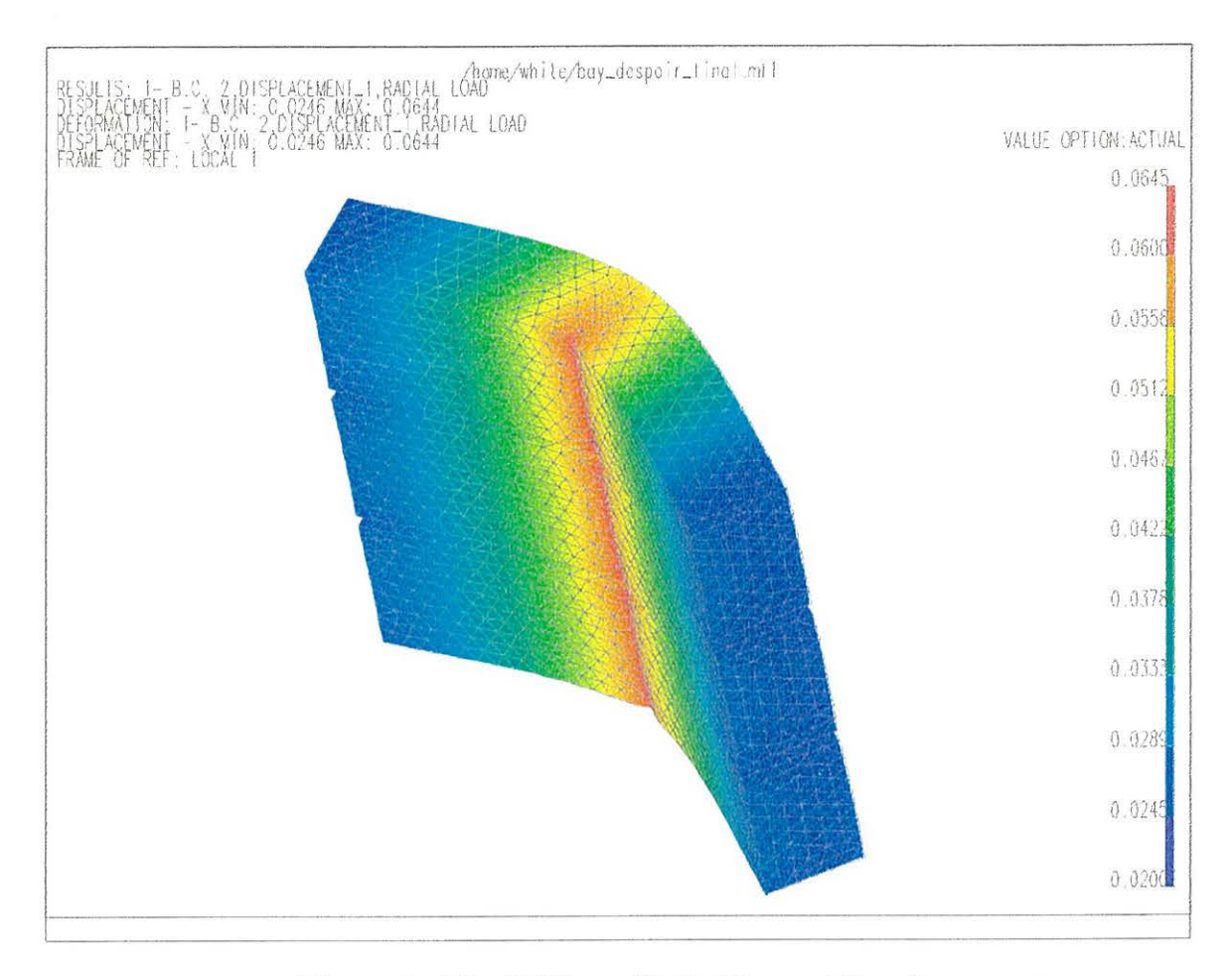


Figure 1: Rim Stiffness Finite Element Results

Figure 1: Rim Stiffness Finite Element Results shows the radial deflection of the rim discs when a load of $10x10^6$ [lbf] is applied at the centre of the disc section. Because there are 8 arms on the rotor spider, a 45° section of the rim was analysed with symmetric boundary conditions applied to the edges of the section.

In can be seen from the finite element results shown in Figure 1: Rim Stiffness Finite Element Results that the radial deflection of the rim was 0.0644 [in] when a radial load of $10x10^6$ [lbf] was applied to the centre of the disc section. Since this deflection is very close to the predicted deflection of 0.0629 [in] for a rim with stiffness of $159x10^6$ [lbf/in], it is concluded that the finite element model of the discs are a realistic representation of the actual rim.

4. Shrink Temperature Difference for Rim

The shrink on the rotor spider is simulated by reducing the temperature of the rim relative to that of the spider so that the interference between the rotor spider and rim at standstill is 0.054 [in] (see section 2.1 Radial Interference Between Rim and Spider Due to Shrink).

Rim Dimensions

D_{orim}:=258.742in

Rim Outer Diameter

DEPTH rimgross := 21.000 in

Average Gross Rim Depth

 $\Delta R_{rim} := 0.054 in$

Radial Expansion of Rim Needed to Provide the Required Interference at Standstill

Properties of Steel

$$\alpha_{\text{steel}} = 1.17 \cdot 10^{-5} \cdot \frac{1}{K}$$

Coefficient of Thermal Expansion for Steel

Determine outside and inside radius of rim.

$$R_{\text{orim}} := \frac{D_{\text{orim}}}{2}$$

 $R_{orim} = 129.371 \circ in$

R_{irim}= 108.371oin

Temperature difference between rim and rotor spider to provide the required interference at standstill.

$$\Delta R = \alpha \text{ steel } R \text{ irim} \Delta T$$

$$\Delta T := \frac{\Delta R_{rim}}{\alpha_{steel} \cdot R_{irim}}$$

 $\Delta T = 42.589 K$

In order to provide the required radial interference between the rim and rotor spider at standstill for shrink up to 115% of rated speed, the temperature of the rim must be 42.6°C below that of the rotor spider.

Figure 2: Finite Element Results for Rim 42.6°C Cooler than Spider shows the results of a finite element analysis where the rim discs were cooled by 42.6°C.

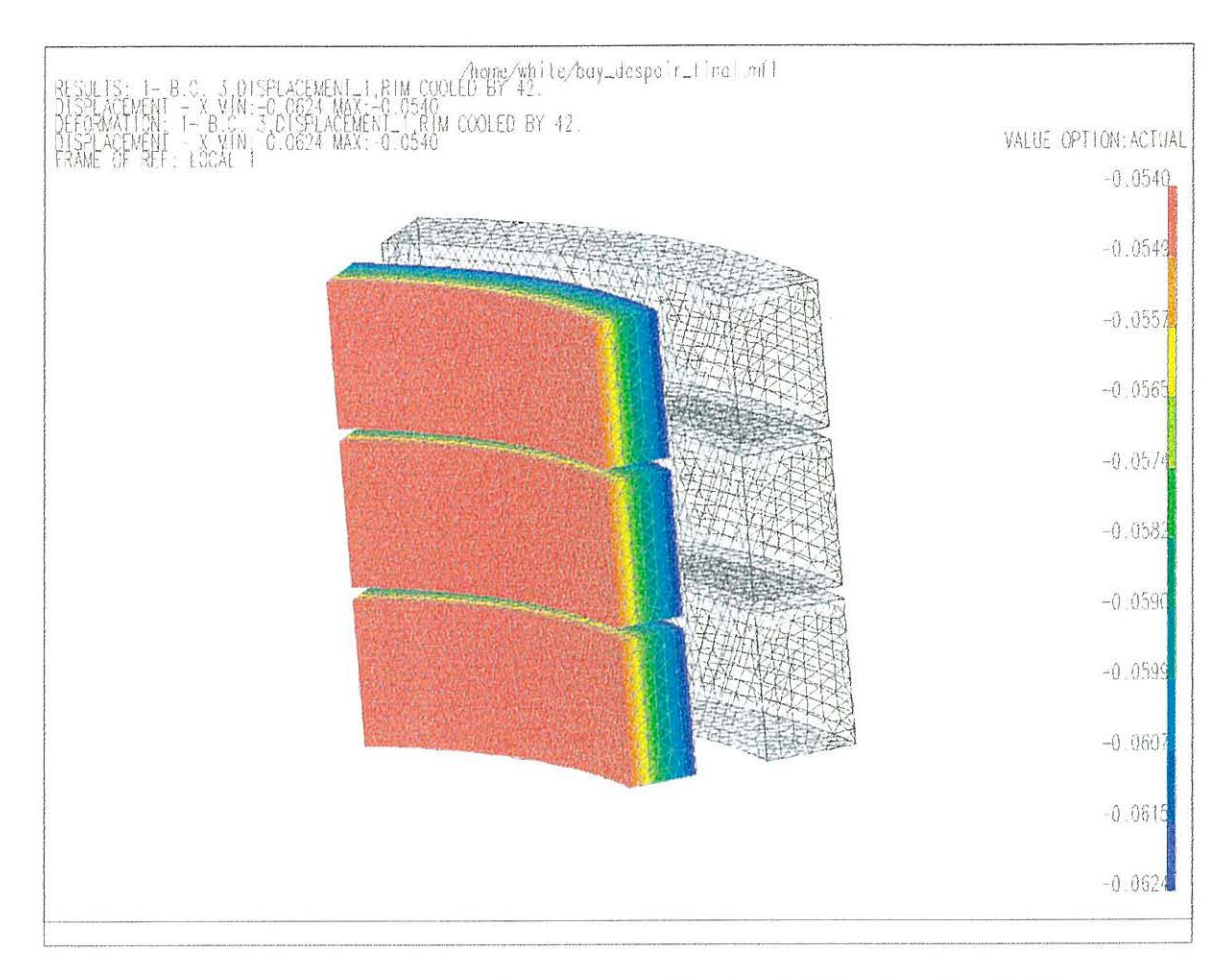


Figure 2: Finite Element Results for Rim 42.6°C Cooler than Spider

Figure 2: Finite Element Results for Rim 42.6°C Cooler than Spider indicates, as expected, that a reduction in the temperature of the rim by 42.6°C produces an inward radial deflection of 0.054 [in] at the inner radius of the rim.

5. Combined Rotor Spider and Rim Finite Element Model

5.1. Geometry of Combined Rotor Spider and Rim Model

Figure 3: Rotor Spider and Rim Finite Element Model shows the section of the combined rotor spider and rim finite element model used for rim shrink analysis. The three rim donuts are located outside of the rotor spider. Tapered cross keys between the arm block on the rotor spider and the rim are shown in the gap between the spider and the rim. These cross keys are required because the arm block on the spider is not machined and, as such, does not provide a suitably flat surface along the axial length of the rim for the transmission of shrink forces. Instead, these forces are transmitted locally by these cross keys. Poles are included outside of the rim to provide

continuity between the three rim donuts. The pipes between the I-beams and the main webs on the actual rotor spider were not included in the finite element model because of difficulty in meshing these components. This is not a concern, however, because these pipes provide negligible radial stiffness to the spider. A large cylinder is located underneath the outer disc on the lower foot of the spider. The purpose of this disc is to prevent a differential deflection of the foot disc in the axial direction, since this type of deflection cannot occur in the rim. In order to accomplish this, the lower cylinder was defined using an orthotropic material that prevents bending in the axial direction but, at the same time, does not provide resistance to bending in the other directions. The axial load due to the rim and poles is applied to the bottom of this cylinder.

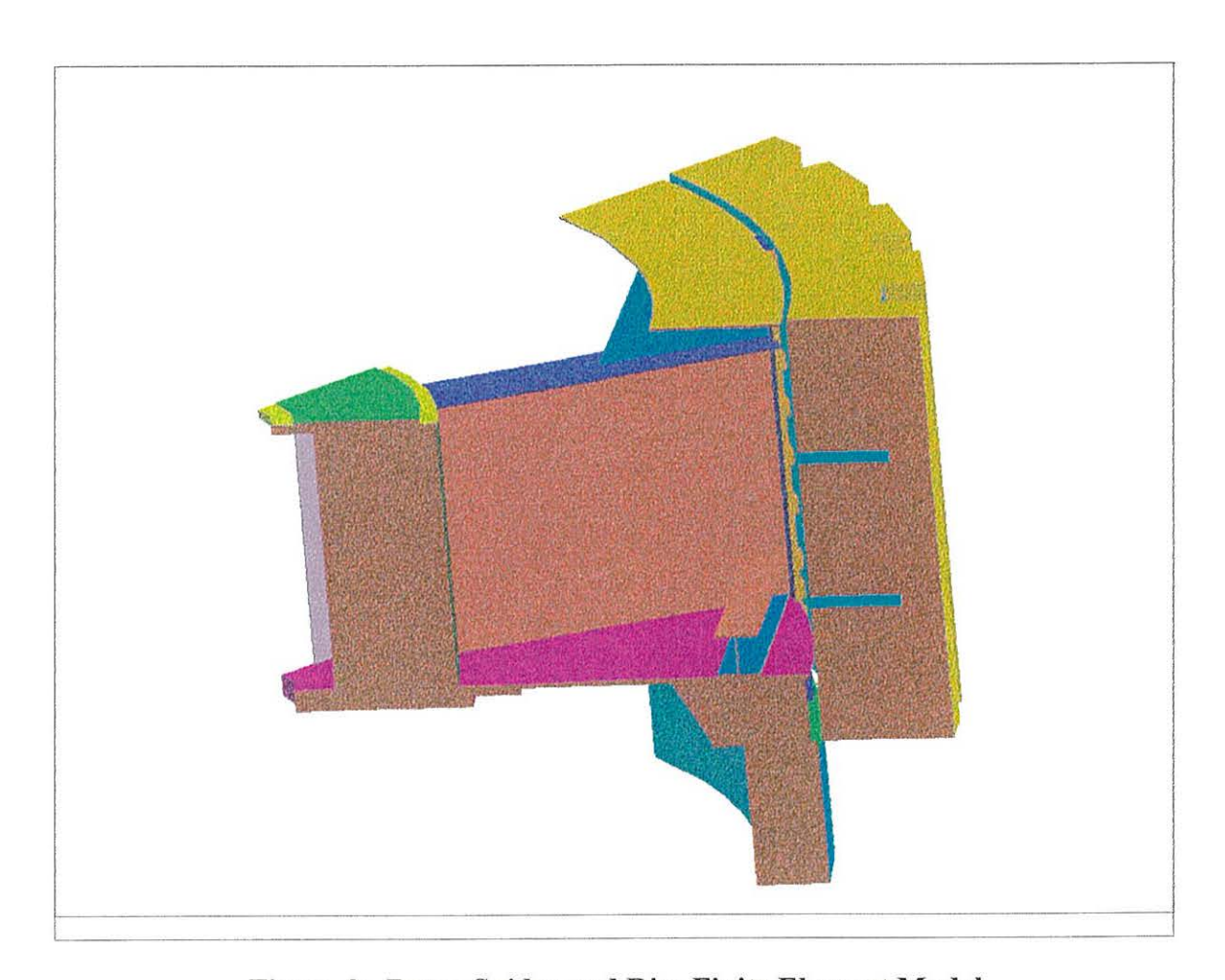


Figure 3: Rotor Spider and Rim Finite Element Model

5.2. Boundary Conditions for Finite Element Analysis

Unless otherwise stated the following boundary conditions were used for each finite element analysis included in this report:

- An axial load of 60,987 [lbf], which represents the weight of the rim and poles, was applied to the rotor spider section. For the case of buckling analyses this load was applied directly to the outer foot disc on the spider. For all other analyses, this load was applied to the bottom of the cylinder positioned underneath the outer foot disc.
- The standstill rim shrink interference of 0.054 [in] was simulated by lowering the temperature of the rim and poles 42.6°C below that of the rotor spider.
- Symmetric boundary conditions were applied to the edges of the rotor spider section. These boundary conditions prevent translation in the θ-direction, and prevent rotation in the r-direction and z-direction.
- The spider was fixed from rotation and translation in all directions, except for radial translation, at the load ring. The load ring is directly underneath the main spider cylinder.

6. Standstill Buckling Analysis

6.1. Standstill Buckling Analysis of Existing Rotor Spider

A buckling analysis of the existing rotor spider at standstill was performed to assess the ability of the spider to withstand buckling due to shrink forces. The results of this finite element analysis, which for clarity only includes the rotor spider portion of the model, are shown in **Figure 4: Buckling Analysis of Existing Rotor Spider at Standstill**.

Figure 4: Buckling Analysis of Existing Rotor Spider at Standstill shows that the top disc of the existing rotor spider will buckle when the rim is shrunk to 115% of rated speed. For the existing spider the buckling load factor, or factor of safety for buckling, is 0.37. Therefore, it is concluded that buckling stiffeners must be added to the existing rotor spider in order to accommodate rim shrink.

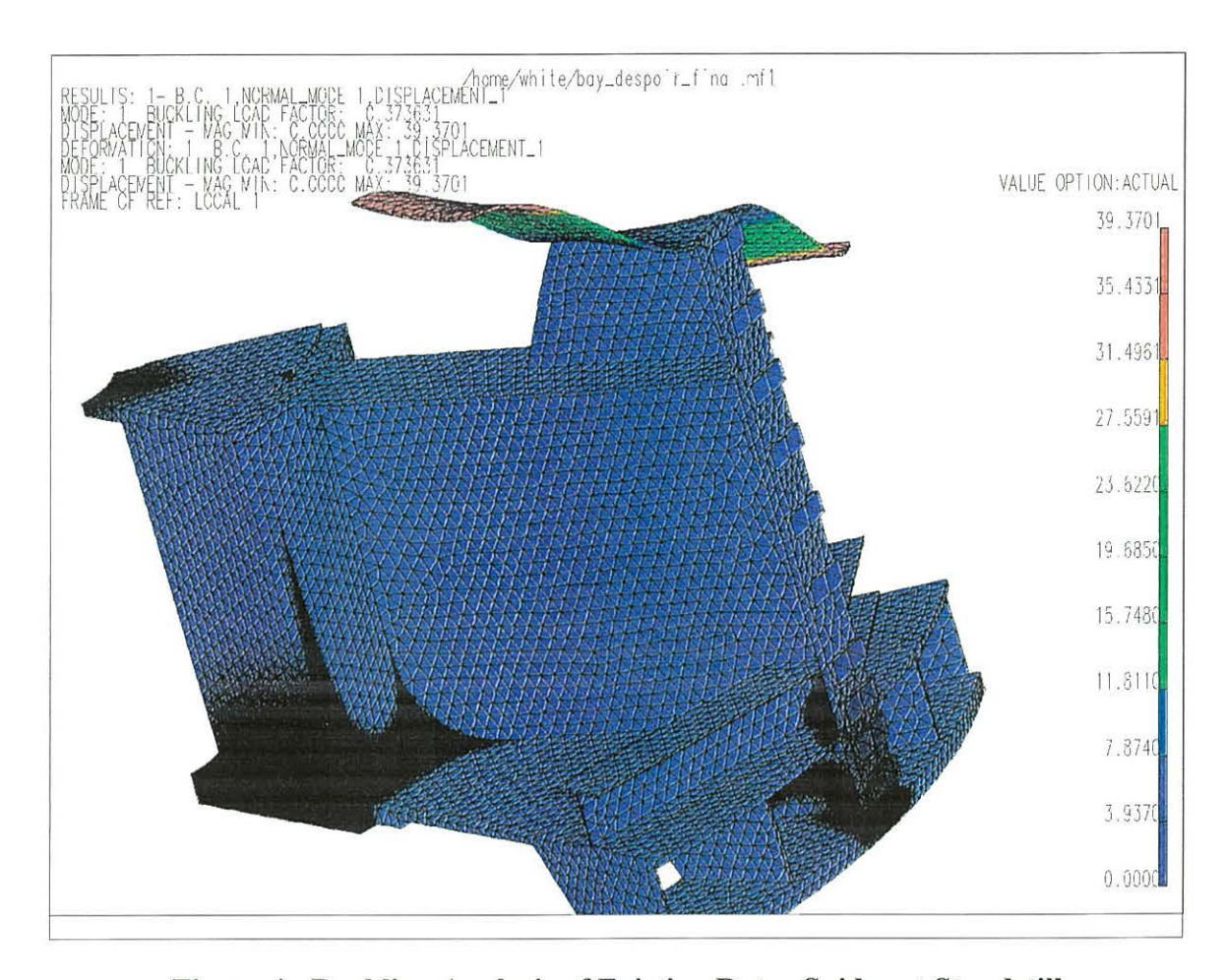


Figure 4: Buckling Analysis of Existing Rotor Spider at Standstill

6.2. Addition of Shrink Angles to Rotor Spider

To provide a sufficiently high factor of safety for buckling during rim shrink, angle supports were added to the spider. A series of finite element analyses were performed, and it was determined that both vertical and horizontal angle supports are required to prevent buckling. 4.00 [in] x 4.00 [in] x 0.375 [in] angle supports are required in both the vertical and horizontal orientations. The inside diameter of the horizontal support is 180 [in], while the inside diameter of the vertical support is 150 [in]. Figure 5: Rotor Spider and Rim Finite Element Model With Shrink Angles shows the solid model of the spider and rim including the angle supports that was used for finite element analysis.

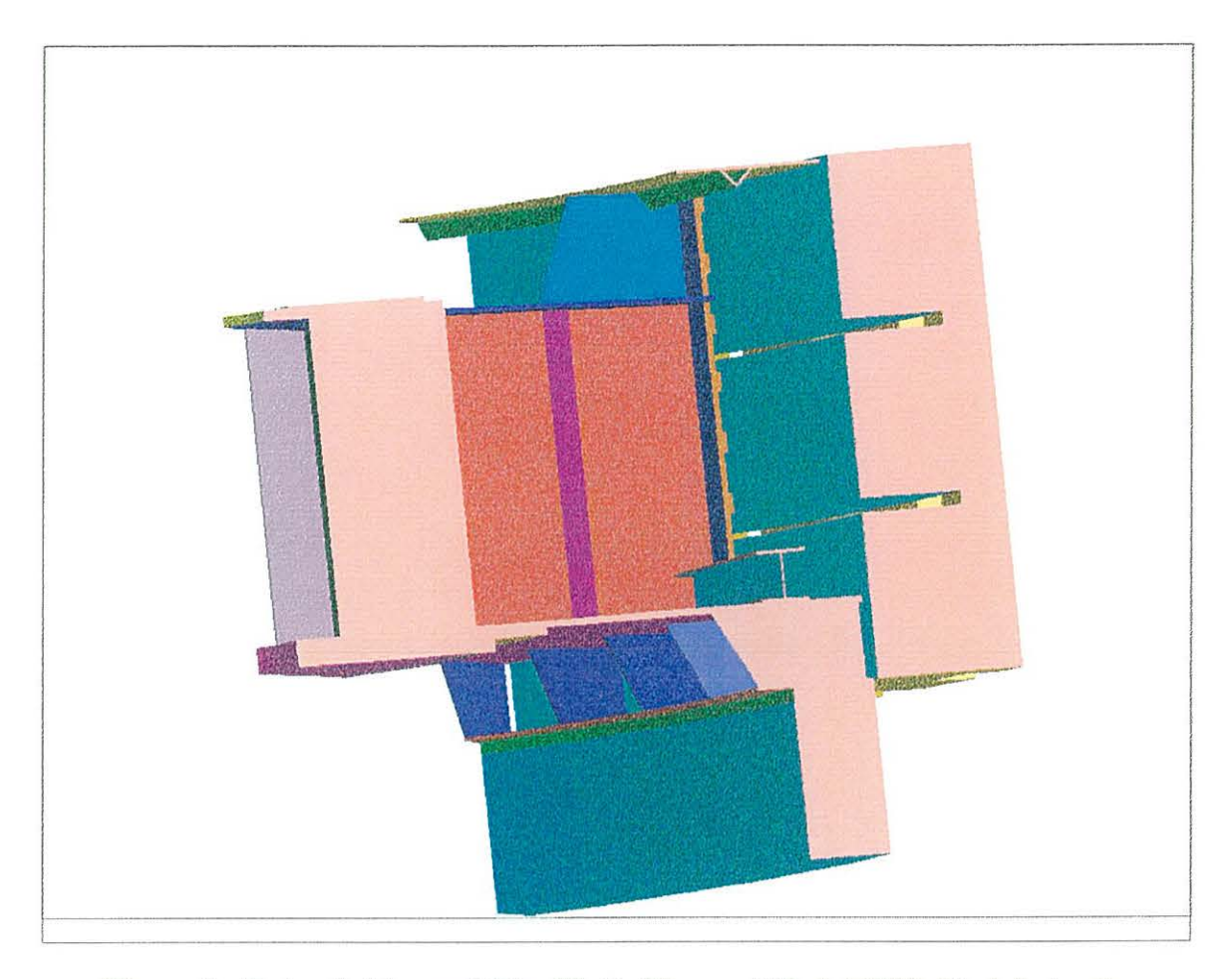


Figure 5: Rotor Spider and Rim Finite Element Model With Shrink Angles

6.3. Standstill Buckling Analysis of Modified Rotor Spider

A buckling analysis of the modified rotor spider at standstill was performed to assess the ability of the spider to withstand buckling due to shrink forces. The results of this finite element analysis, which only includes the rotor spider portion of the model, are shown in Figure 6: Buckling Analysis of Modified Rotor Spider at Standstill.

Figure 6: Buckling Analysis of Modified Rotor Spider at Standstill indicates the factor of safety is 2.32 against buckling of the modified rotor spider at standstill for rim shrink to 115% of rated speed.

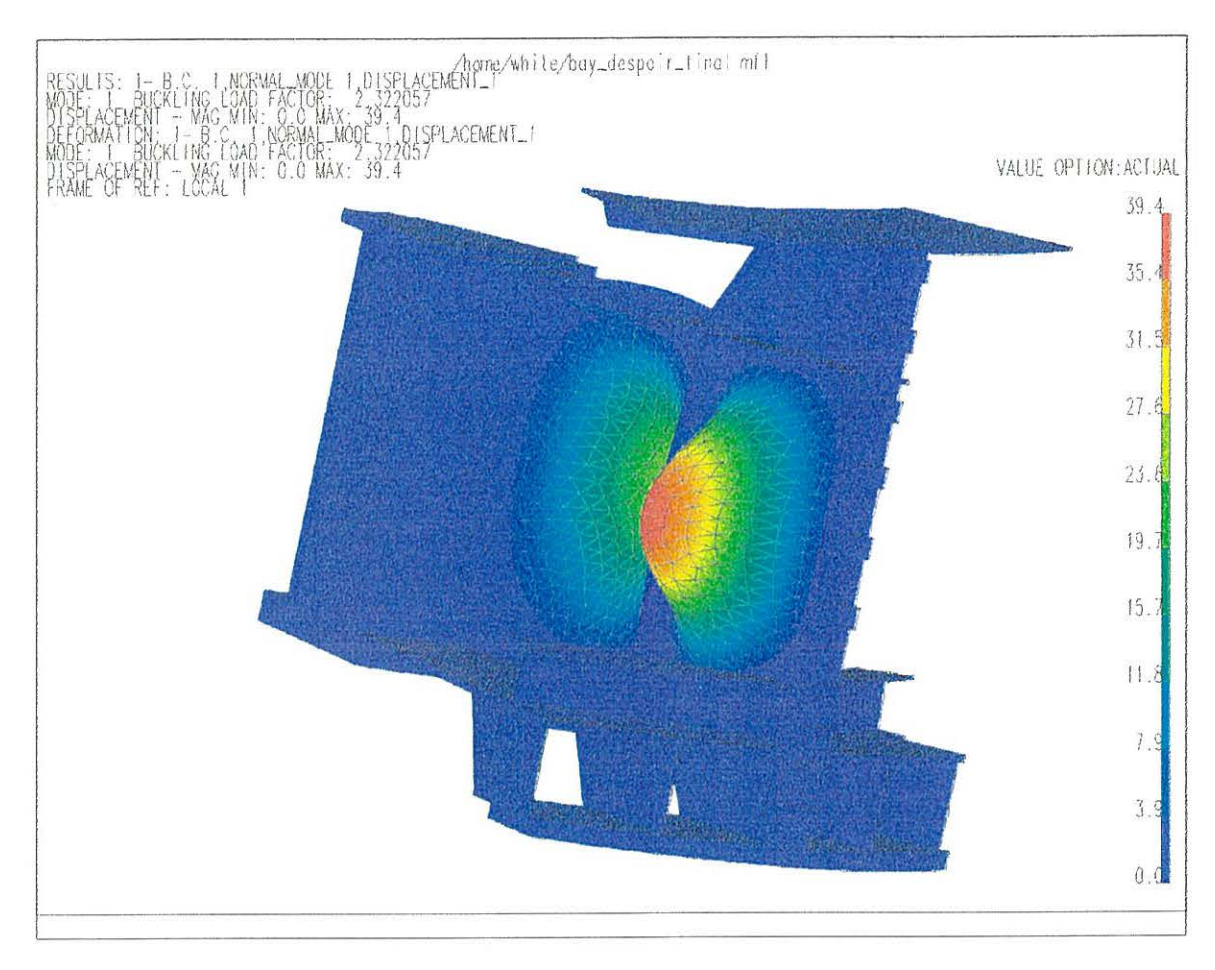


Figure 6: Buckling Analysis of Modified Rotor Spider at Standstill

7. Final Rotor Spider Dimensions

As a result of the buckling analysis performed on the rotor spider, it was concluded that vertical and horizontal 4.0 [in] x 4.0 [in] x 0.375 [in] shrink angles are required. Also, tapered cross keys are required since the arm blocks on the existing rotor spider do not provide a flat surface against which the rim can be shrunk. **Figure 7: Cross Key and Angle Support Dimensions** shows the required dimensions and locations for the cross keys and the angle supports.

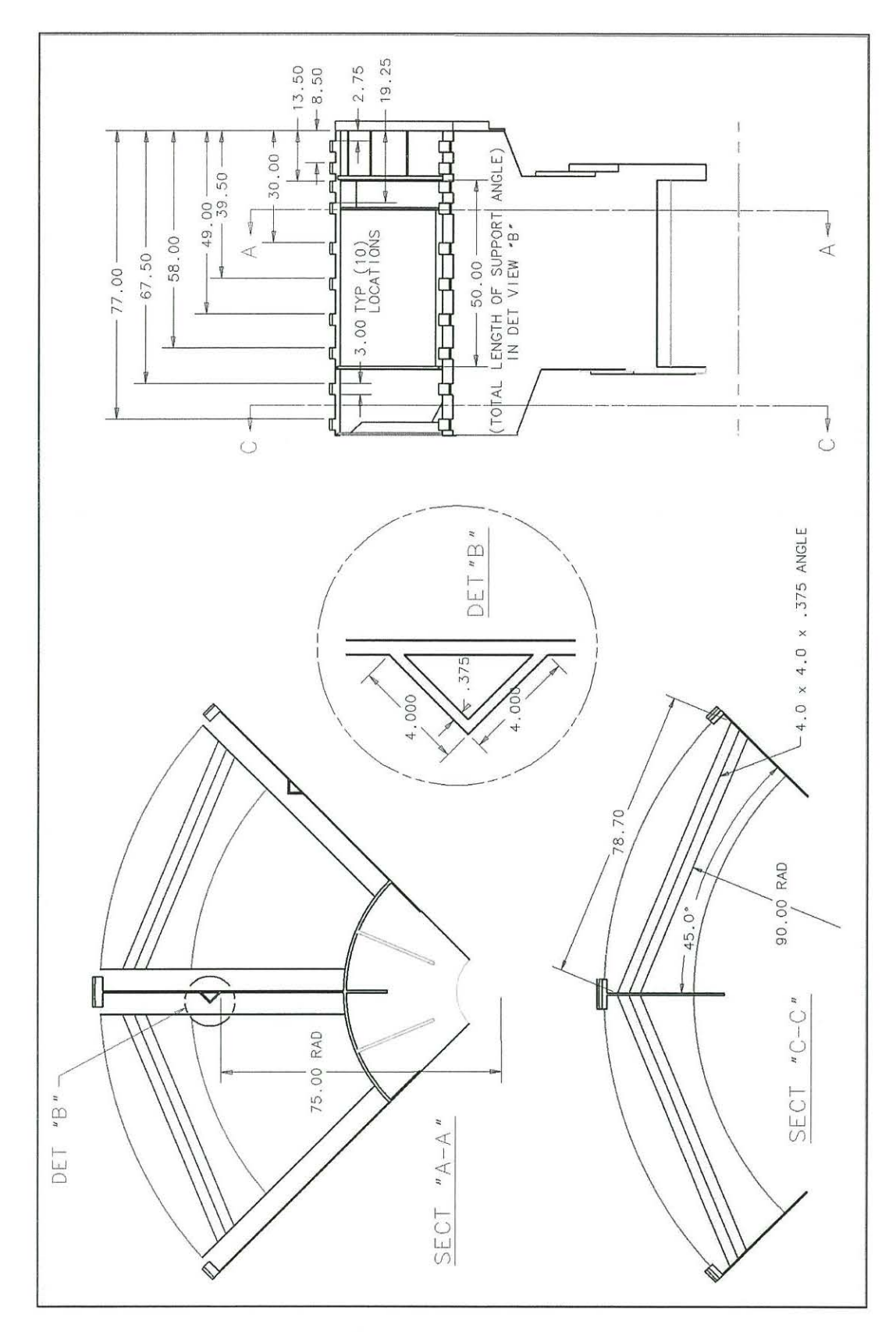


Figure 7: Cross Key and Angle Support Dimensions

8. Structural Analysis of Spider at Standstill Due to Shrink

This section deals with the analysis of the final rotor spider for stresses, deflections, and forces due to rim shrink.

8.1. Deflection of Rotor Spider at Standstill Due to Shrink

Figure 8: Deflection of Spider at Standstill Due to Shrink and Figure 9: Radial Deflection of Spider at Standstill Due to Shrink show the deflection of the rotor spider at standstill due to the forces generated during rim shrink. Figure 9: Radial Deflection of Spider at Standstill Due to Shrink indicates that the radial deflection at the inside of the bottom disc on the rotor spider is approximately 0.003 [in]. Because this deflection is so low, difficulties in uncoupling the rotor spider from the shaft are not anticipated following rim shrink since the clearance between the coupling studs and the coupling stud holes is 0.0055 [in].

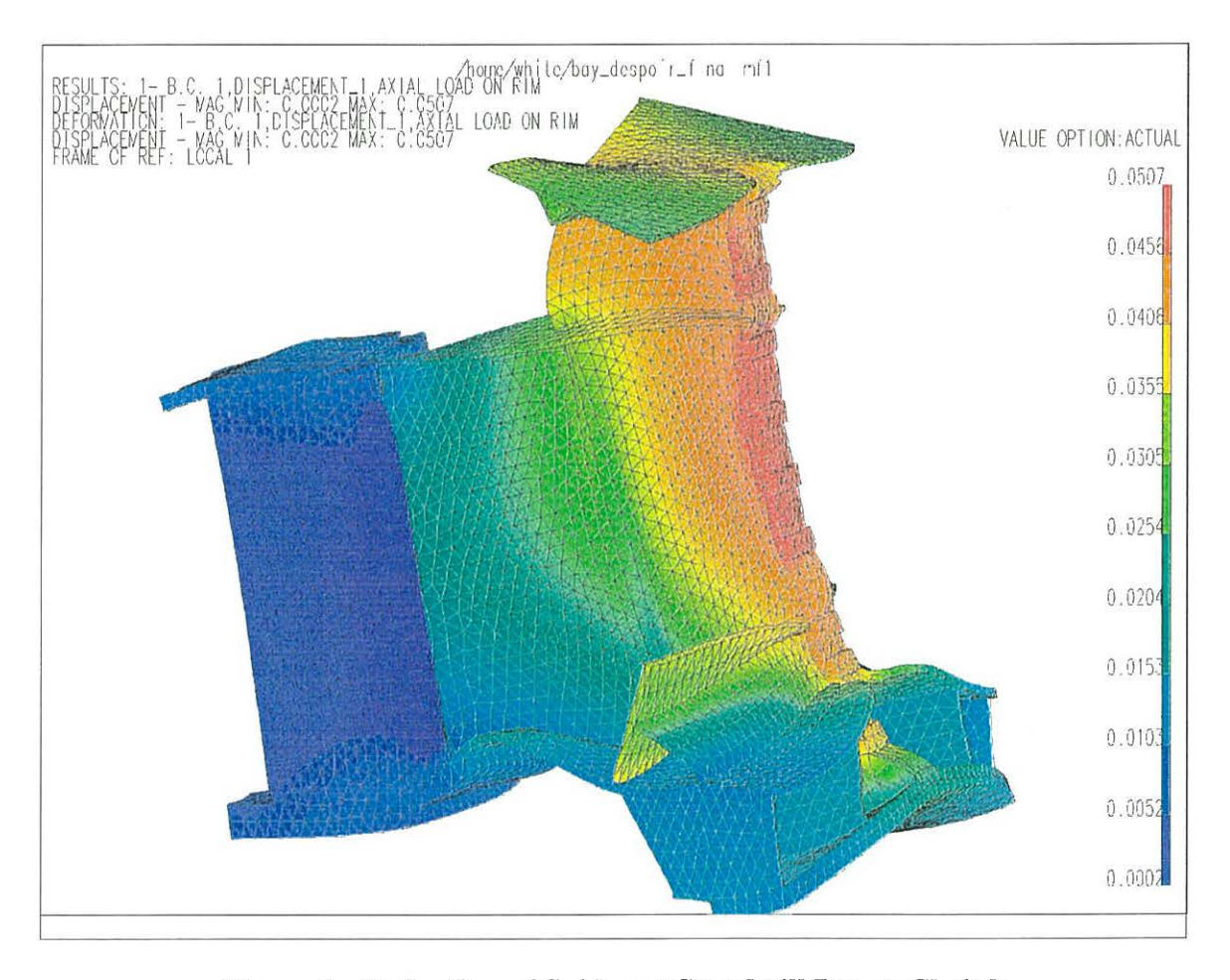


Figure 8: Deflection of Spider at Standstill Due to Shrink

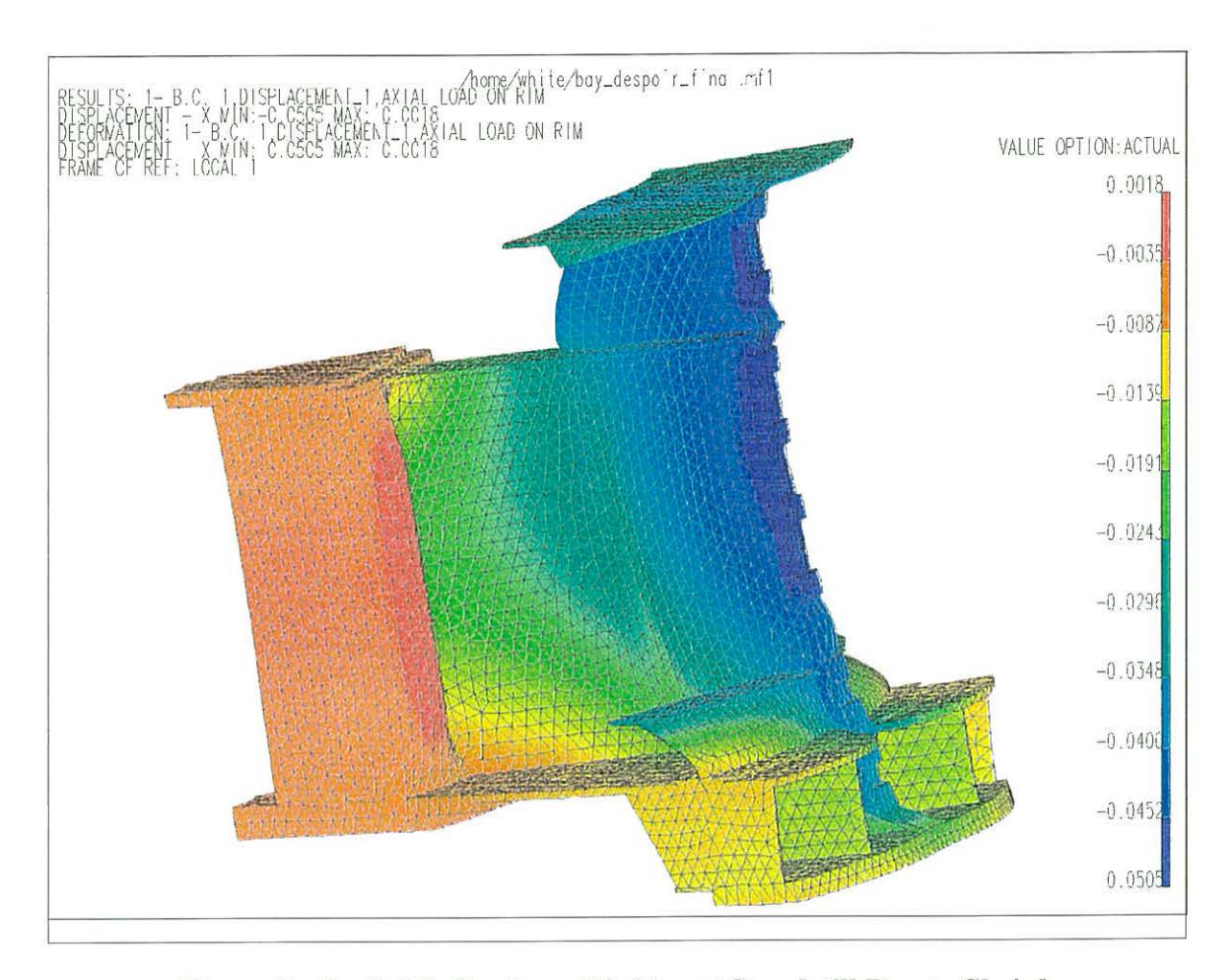


Figure 9: Radial Deflection of Spider at Standstill Due to Shrink

8.2. Stress in Rotor Spider at Standstill Due to Shrink

The material in the rotor spider is equivalent to ASTM A36, which means it has a yield strength of 36,000 [psi] and an ultimate strength of 68,000 [psi]. Figure 10: Von Mises Stress Up to 36,000 [psi] in Rotor Spider and Figure 11: Von Mises Stress Up to 68,000 [psi] in Rotor Spider show the Von Mises stress in the rotor spider at standstill due to rim shrink to 115% of rated speed. In these figures, stresses beyond the upper limit are black.

Figure 10: Von Mises Stress Up to 36,000 [psi] in Rotor Spider shows the stress up to the yield strength of the material. Stresses beyond this point are shown as dark patches on the finite element model. From the finite element analysis, it is seen that several locations on the rotor spider will be stressed beyond the yield point of the material. The primary locations of high stress include the joint between the arm block and the outer bottom disc, and the webs directly behind the arm block near the outer bottom disc. Therefore, some local yielding of the rotor spider near the joint between the arm block and outer bottom disc is expected when the rim is shrink to 115% of rated speed. It should, however, be noted that the amount of material in the spider

that is stressed beyond the material yield is relatively small, thus, not adversely reducing the effectiveness of the proposed shrink.

The amount of plastic deformation in the rotor spider is comparable to the levels of deformation predicted by similar analyses on existing hydroelectric generators of shrunk-rim design. In particular, stresses in the rotor spider for the Itumbiara generating station were predicted to be very similar to those predicted for the Bay D'Espoir rotor spider in terms of stress level and The Itumbiara rotor spider is similar in design to the Bay D'Espoir spider in that they both have intermediate discs that end in radially deep spokes, and an outer disc at the top of the spider. It has been 20 years since the rims at Itumbiara were shrunk for the purpose of maintaining the roundness of the rotor. In this time no problems regarding rim shrink on these spiders, in terms of vibration or rotor roundness, have been brought to our attention. Therefore, it is felt that the Itumbiara rotor spiders have been able to provide sufficient rotor stiffness to prevent rotor shape and centring problems, despite the high levels of stress predicted in these components due to rim shrink. As a result of the similar stress patterns seen in the Bay D'Espoir and Itumbiara rotor spider analyses, the proposed rim shrink on Bay D'Espoir should be adequate to maintain rim concentricity, thereby eliminating rotor balance problems.

A god sign

Figure 11: Von Mises Stress Up to 68,000 [psi] in Rotor Spider shows the stress in the rotor spider up to the ultimate strength of the material. Stresses beyond the ultimate limit are shown as dark patches on the finite element model. Small areas of stress beyond the ultimate limit are seen at the joint between the arm block and the outer disc. These areas of stress are very local, and come about because of the assumption that the stress-strain curve remains linear. This is not the case. In actuality, these areas of high stress will deform at a much lower stress level, which will cause the load to be absorbed by the surrounding material at a stress level below the ultimate limit. Therefore, failure of the material in these locations is not anticipated. As a final note in this regard, finite element analysis of rim shrink on the Itumbiara rotor spider revealed local stresses at the joint between the arm block and the outer bottom disc exceeding the ultimate material strength. Because these machines have been in service for some time without any indication of problems related to rim shrink, stresses beyond the ultimate material limit predicted for the Bay D'Espoir rotor spider are not an indication that rim shrink poses a threat to the structural integrity of the spider.

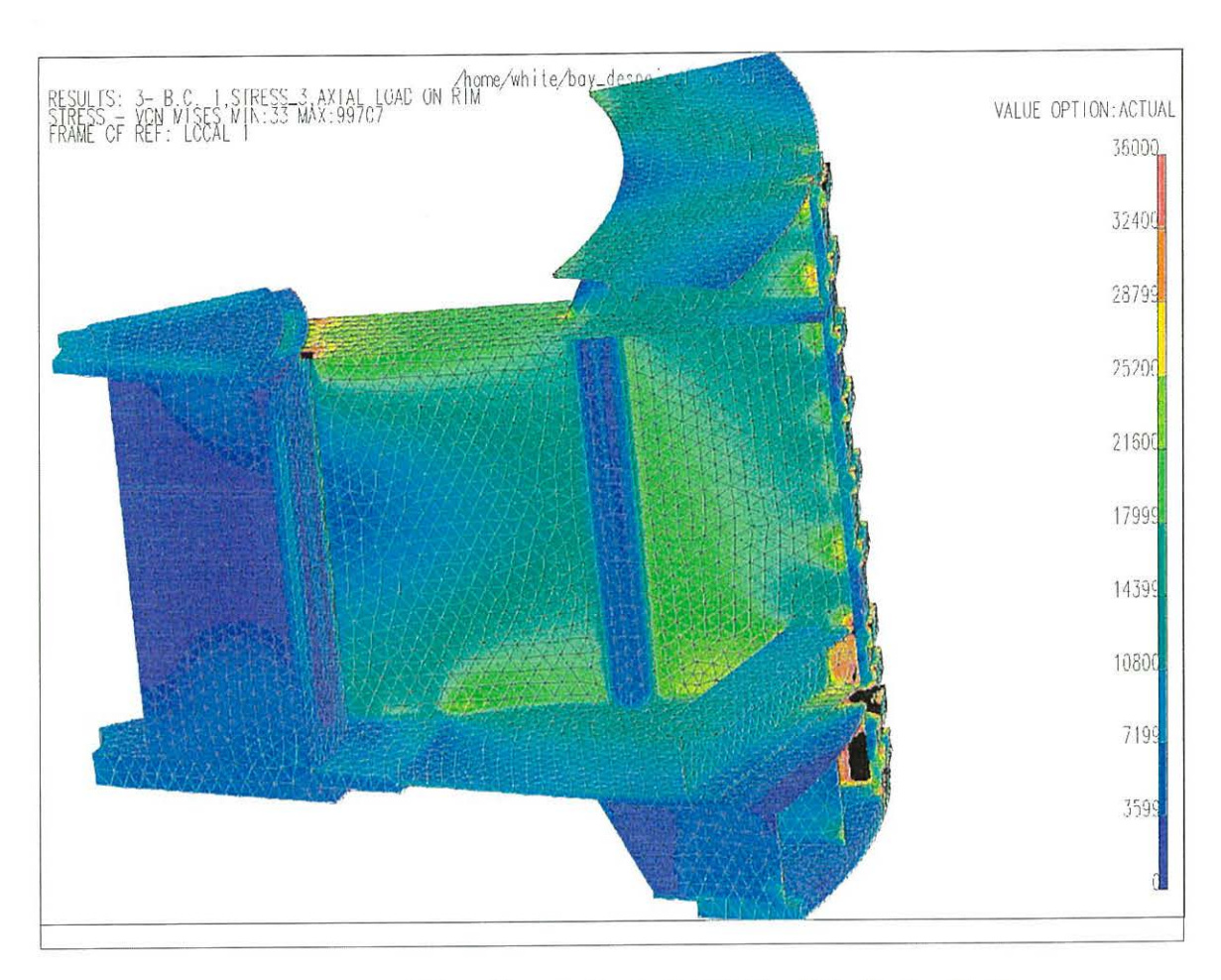


Figure 10: Von Mises Stress Up to 36,000 [psi] in Rotor Spider

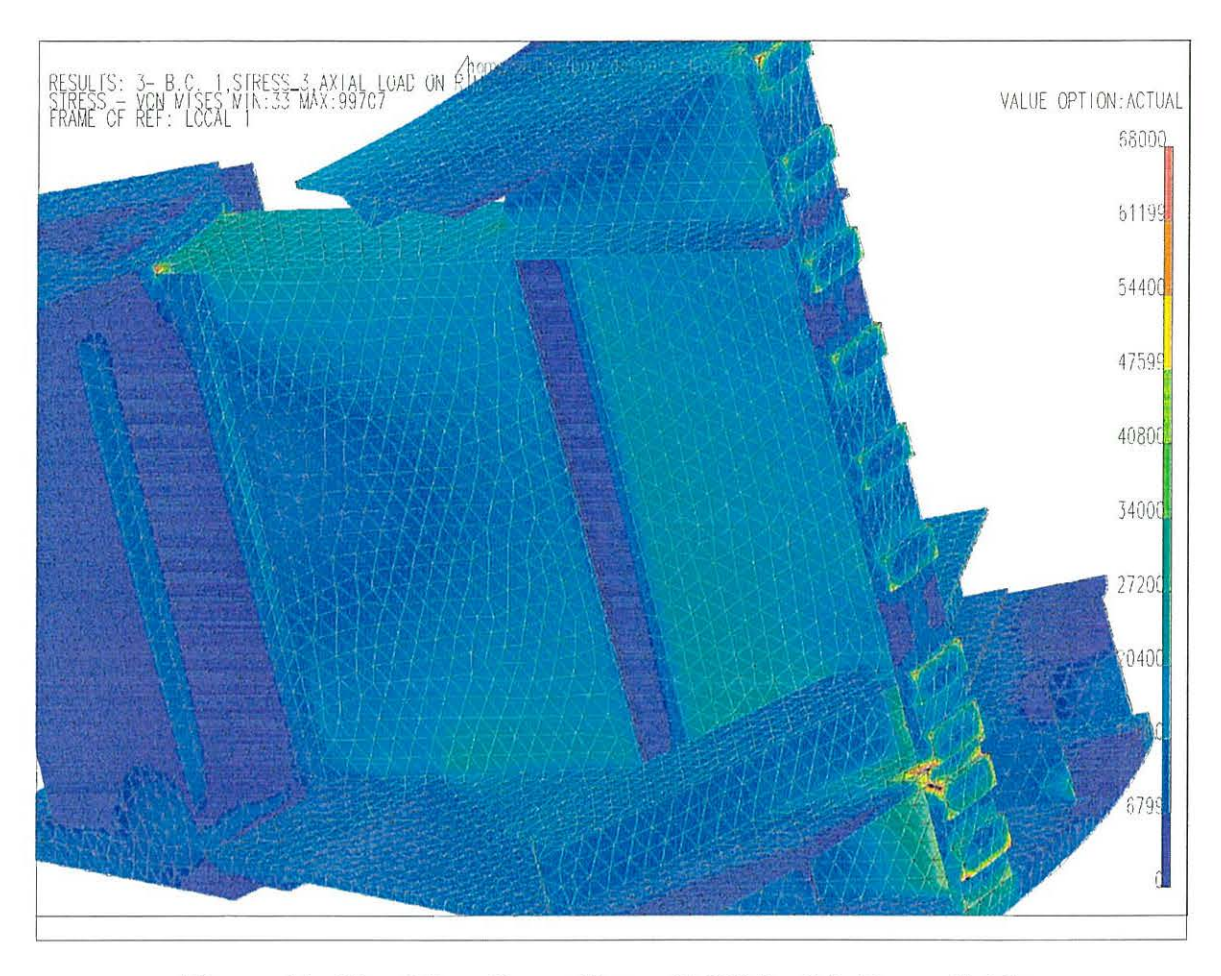


Figure 11: Von Mises Stress Up to 68,000 [psi] in Rotor Spider

8.3. Radial Force on Rotor Spider at Standstill Due to Shrink

Radial forces between the rim and rotor spider during rim shrink were determined using two successive finite element analyses. In the first analysis, the rim was cooled to simulate shrink and the deflection of the rotor spider at each cross key was determined. A subsequent finite element analysis was performed on a model of the rotor spider that did not include the rim. For this analysis the radial deflection of each cross key, determined in the previous analysis, was applied to the keys on the spider. The radial force between the rim and the rotor spider was determined as the reaction force required to bring about the corresponding radial displacement at the cross key. The following table summarises the radial deflection and force at each cross key (where cross key 1 is at the top of the arm block):

| Cross Key Number | Radial Deflection [in] | Radial Shrink Force [lbf] |
|------------------|------------------------|---------------------------|
| 1 | 0.046 | 121,100 |
| 2 | 0.049 | 100,500 |
| 3 | 0.050 | 135,400 |
| 4 | 0.050 | 85,420 |
| 5 | 0.050 | 104,000 |
| 6 | 0.048 | 113,100 |
| 7 | 0.044 | 164,100 |
| 8 | 0.040 | 325,000 |
| 9 | 0.038 | 319,700 |
| 10 | 0.035 | 168,200 |
| TOTAL | - | 1,636,520 |

The radial shrink force between the rim and each arm on the rotor spider, as determined using finite element analysis, is 1.6×10^6 [lbf].

9. Recommendations for Rim Shrink

Provided a vertical angle support is added to the each arm main web, and a horizontal stiffener is added to the upper disc between arm webs, it is feasible to shrink the Bay D'Espoir 7 rotor spider to 115% of rated speed. Based on the results of several finite element runs, it is concluded that the modified rotor spider will not buckle due to shrink forces, and the stresses in the spider will be acceptable following rim shrink. Furthermore, with this level of shrink, the spider will be able to be uncoupled from the shaft without heating the rim due to the small radial deflection of the inner bottom disc that is caused by rim shrink forces.

10. Rim Shrink Procedure

This procedure is a general guideline and certain details might not be suitable for all rim shrinks.

- 1. Obtain the electrical equipment that will be required for the heat shrink. Ensure that the quantity and type of heater is satisfactory, thermal insulated wire size is adequate and that circuit breakers and transformers are of sufficient ratings. Similarly, ensure that suitable insulating blankets, connectors, etc. are available. "Try to minimise the number of electrical connections required."
- Perform a standard rotation check and plot the rotor roundness on polar paper to aid in visualising the rim shape. See Figure 12: Rotor Position and Key Movements.
- 3. Plot the top and bottom average radius on polar paper to determine which direction the rim would have to move in relation to each spider arm in order to bring the rim to the average rim radius. For this the horizontal key movement that will be required during the heat shrink can be determined.

e.g. HORIZONTAL KEY TAPER 0.250/ft Choose a particular spider arm that you want to move Top of Rim OUT 0.020 [in] Bottom of Rim IN 0.010 [in]

To match the corresponding top and bottom average radii: Move top key IN 1 [in] and bottom key OUT 0.5 [in]. For aid in visualising effect of key movement consider key IN as positive and key OUT as negative reactions.

- 4. Determine the required key moves for the top and bottom horizontal keys for all spider arms. Check the integrity of the planned moves using Positive-Negative reaction; the sum of all moves should be roughly zero.
- 5. Having established the top and bottom key moves, the remaining horizontal key moves can be determined. Assuming that the rim profile is nearly linear and that there is roughly equal horizontal key spacing the spider arm key moves as in the example would be as follows,

| Top Key Number | Arm Key Move [in] | Bottom Key Number | Arm Key Move [in] |
|-------------------|----------------------|----------------------|----------------------|
| 1 | +1.0 | 1 | -1.0 |
| 2 | +0.7 | 2 | -0.7 |
| 3 | +0.4 | 3 | -0.4 |
| 4 | +0.1 | 4 | -0.1 |
| 5 | -0.2 | 5 | +0.2 |
| 6 | -0.5 | 6 | +0.5 |
| Sum | +1.5 | Sum | -1.5 |

NOTE

Extreme out-of-roundness, where the radial out-of-roundness is larger than the thickness of the heat shrink shims should be handled differently.

- 6. Install the stationary heat shrink keys and the vertical drive keys. At each spider arm location temporary hold-up tabs may be required on both the stationary and vertical drive keys depending on the type of rim support block arrangement. See **Figure 13: Typical Heat Shrink Key Arrangement**. If the stationary or vertical drive key in this sketch were allowed to drop, their tapered corner would ride on a square corner and they might become skewed. The hold up tab on the vertical drive key serves another purpose in that the key has to be lifted during the heat shrink and will return to the set tab elevation upon completion of the heat shrink.
- 7. Start installing the horizontal drive keys into position, ensuring that the stationary and vertical drive keys are properly engaged. When installing the horizontal keys try to leave sufficient key sticking out past the edge of the spider

arm block to allow for the appropriate key movement, key sledging and adequate room for final welding.

e.g. If a particular key has been identified as having to move in 1 [in], try to leave 2 [in] or more sticking out when the key is inserted by hand. The key might drive up to 0.5 [in]. The heat shrink will require that the key be moved 1 [in]. A second heat may be required which might mean that this key has to be moved further, and finally there has to be a weld between the key and the spider arm.

For the first heat assume a key taper to rim movement ratio of one to one. The spider might go into plastic compression, which would result in the rotor not being as round as anticipated and a second heat might be required.

NOTE

The variety of original horizontal key sizes will probably not be adequate. This implies that part of the keys supplied will have to be machined to provide intermediate size keys so that adequate key movement and key positions will be available. When sizing keys for machining try to minimise that amount of machining and keep in mind that it might be easier to machine the keys twice than to order more raw material. Also, the drawing might ask that all of the horizontal keys be cut off to leave only 2 [in] showing past the edge of the spider arm. Depending on the key sizes and the amount of key movement required, this step might not be practical or possible.

8. With all the horizontal keys secured by hand, they should now be snugged up metal to metal. The first keys to be snugged should be where the rotor rim has to be pushed radially outward the furthest. Sledge these keys until they stop moving. Then snug up the remaining keys with a 2-pound hammer.

NOTE

All of the torque drive keys will have to be refitted, but some keys that have been lubricated with molycote should be left in the blocks in order to avoid having a tangential shift in the rim during the horizontal key sledging and subsequent heat shrink. This might reduce the need for special oversize or undersize torque drive keys.

- 9. With all of the horizontal keys snug, recheck the rotor roundness to see if the sledging has affected the original rotor roundness. A radially "thin" rim will often start to shape change with sledging the keys. It also might be necessary to revise the list of key moves.
- 10. Ensure that the rotor is properly grounded. Assemble the heating system and perform any appropriate test to ensure that the system will work satisfactorily. Measure voltage, resistance and/or current.

All the torque block keys should be removed except for the few mentioned, to stop any tangential shift. The rotor should be coupled to the shaft during the shrink to reduce the effect of possible undulations in the coupling face due to uneven stresses in the spider. Place insulating blankets around rim as required.

11. Record dimensions, set up thermocouples or thermometers and begin heat shrink.

The heat shrink should be started first thing in the morning as the heat time required might be unknown. The first indication of rim growth will be the loosening of the horizontal keys. These keys should not be moved at this time.

Once the vertical drive key is loose, lift it up enough to allow all of the horizontal keys to be adjusted as per the calculated movements.

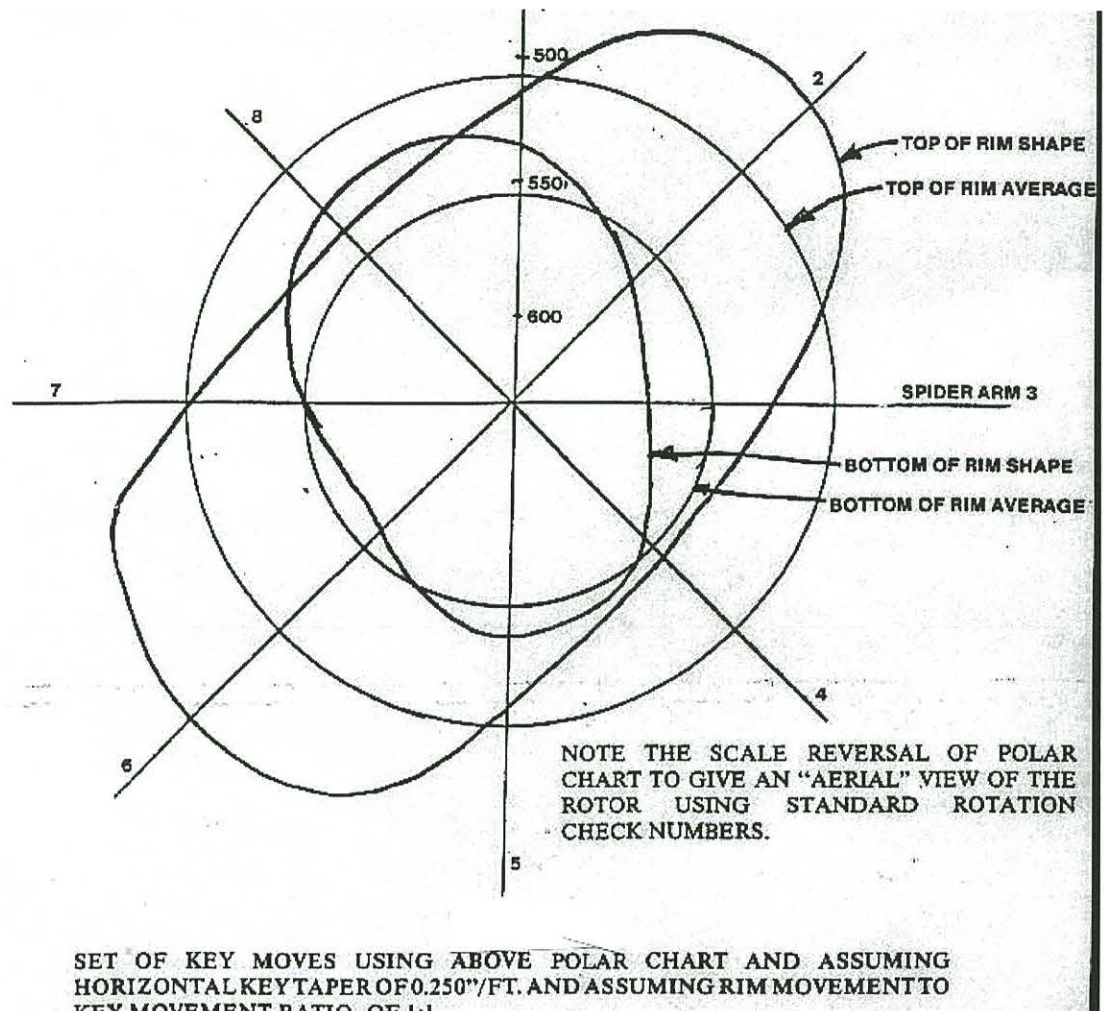
After completing all the horizontal key moves, raise the drive key enough to allow the heat shrink shim to be placed into position, then drop the vertical key back into place. The varying heights of the vertical drive keys, when they are first repositioned, should be a good indication of where the rotor is most out-of-round. These is no point driving the vertical drive keys back into place until ½ or more of them have fallen back to their original position. Driving these keys before then would only aid in conducting the rim heat into the spider.

In the event of blown heater or shorts, shut down the entire system before effecting repairs. Certain electrical problems may be isolated and repaired separately but the heat in the rim should be maintained as uniformly as possible. Do not shut down part of the heat system.

12. When all shims are in place and the vertical drive keys are back at the start position, shut down the heating system and remove any blanketing or insulation and allow the rim to cool down.

During the cool down period (5 to 6 days for a large rim) visually check for any unusual stress build-ups, cracks, bulging or cupping effects on the spider arms or other surfaces. If there is any indication of distress the heat level should be re-applied to reduce the shrink forces and Generator Engineering is to be notified and a course of action outlined.

- 13. When the rotor has returned to room temperature, perform a final rotation check and forward result to Engineering. A second heat may be required to correct any unexpected rim movement. Any further action should be referred to GE Hydro Generator Engineering for approval.
- 14. When an acceptable rotor shape is deemed to have been achieved, the horizontal cross keys on the shrink key assembly shall be welded at both sides of their interface with the rotor spider arm block.



KEY MOVEMENT RATIO OF 1:1

| SPIDER ARM # | 1. | 2 | 3 | 4 | 5 | 6 | 7 | - 8 |
|--------------|---------|---------|--------|--------|--------|---------|---|--------|
| TOP KEY #1 | IN+1/4 | OUT-2.0 | IN+1.2 | IN+2.2 | IN+.25 | OUT-2.7 | 0 | IN+1.7 |
| 2 | +0.1 | -1.5 | +1.2 | +1.8 | +0.05 | -2.1 | 0 | +1.1 |
| 3 | -0.05 | -0.9 | +1.2 | +1.4 | -0.1 | -1.5 | 0 | +0.5 |
| 4 | -0.20 | -0,4 | +1,3 | +1.0 | -0.25 | -0.9 | 0 | -0.1 |
| 5 | -0.35 | 1.0+ | +1.3 | +0.6 | -0.4 | -0.25 | 0 | -0.7 |
| 6 | OUT-1/2 | IN+.7 | IN+1.3 | IN+.2 | OUT6 | IN+.4 | 0 | OUT1.3 |

 Σ OF TOP KEYS = +.25-2.0+1.2+2.2+.25-2.7+0+1.7=0.9" $\Rightarrow 0$ Σ OF BOTTOM KEYS = -1/2+.7+1.3+.2-.6+.4-1.3 = 0.2" = 0

Figure 12: Rotor Position and Key Movements

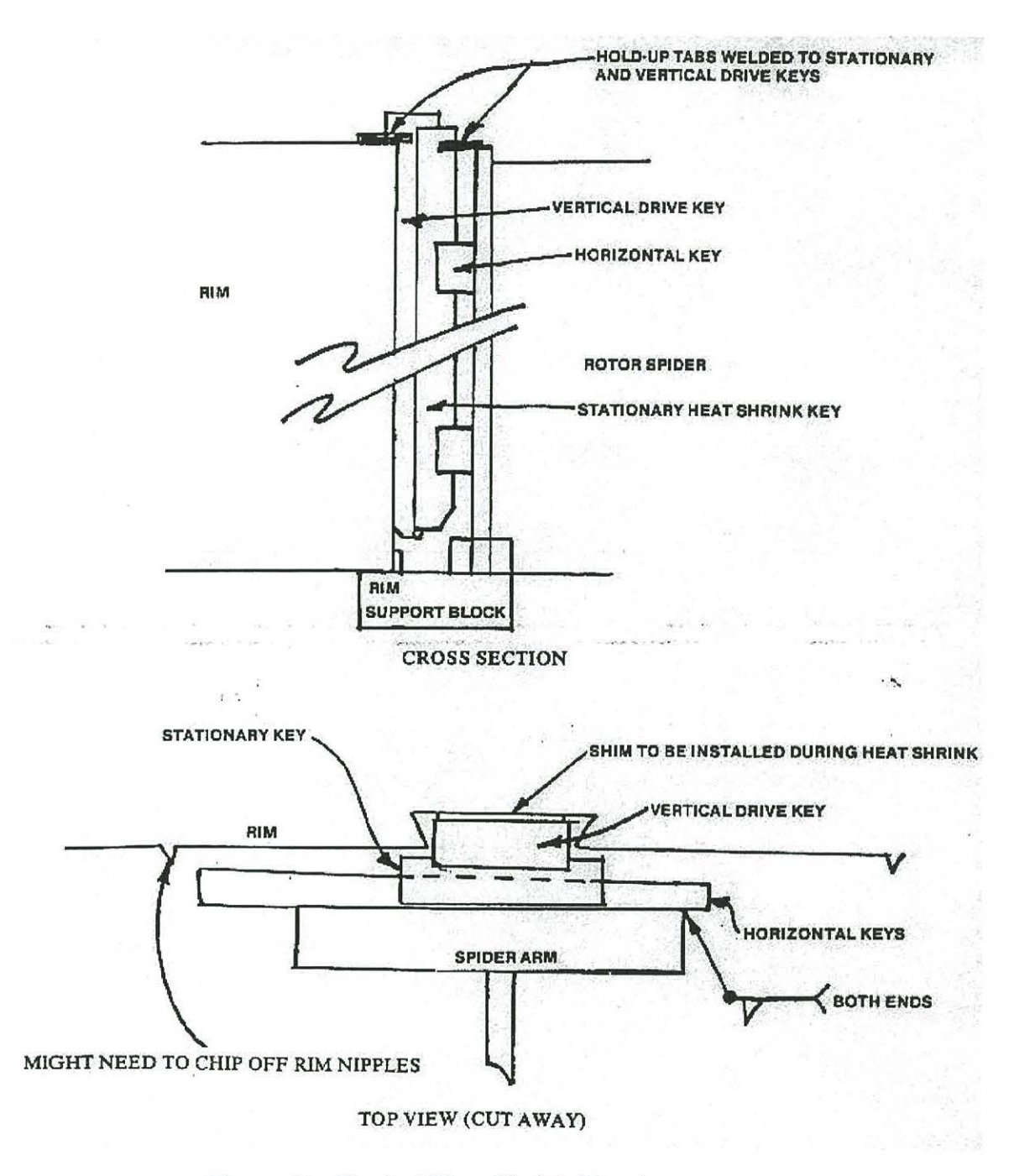


Figure 13: Typical Heat Shrink Key Arrangement

11. Rim Heaters

The existing rotor rim was constructed without a direct means of inserting a straight Calrod type heater into the rim structure. This method is typically used to heat rotor rims to expand them relative to the rotor spider to enable the shrink shims to be inserted. Consequently, an alternative type of heater is recommended.

With the intention of shrinking the rotor rim with the rotor poles in place, there is a somewhat limited availability of locations for the rim heaters. The heaters that GE has deemed most appropriate are strip-type heaters. These heaters would be applied on the inner bore surface of the rim, located at 24 pole centerline sites (8 locations occupied by the rotor spider arm ends). The length of these heaters allow full coverage of each of the 3 rim sections, therefore, requiring 24 x 3 = 72 heaters. Each heater would have a power rating of approximately 3 kW. In addition to these strip heaters, "hair-pin" shaped Calrod type heaters would be inserted between the rim sections at 2 inter-section planes (total of approximately 48 heaters). After installing and connecting the heaters, thermal blankets must be positioned over the heaters to prevent heat loss and to insulate the rotor spider from thermal rise.

The budget price for a set of these heaters is \$18,000 and thermal blankets about \$2000. Along with the above, wiring and a power distribution panel is needed and is not part of the stated budgetary prices.

12. Shrink Keys and Anti-buckling Stiffeners

To modify the rotor spider and rim-to-spider keying system to permit the rim to be shrunk, addition parts must be obtained.

a) Rim Keys

As the rotor spider arm ends were not machined to accommodate a rim shrink, supplementary means must be provided for applying the shrink forces across the spider /rim interface, and at the same time, provide the maximum shape control to the rim. These key assemblies (see Figure 13) consist of several parts including an axial carrier key. This key has horizontal tapered slots at several locations along its length. At each of these slots, a tapered horizontal key is inserted that provides the ability to adjust the radial position of the rim / spider contact point to create a round and vertical cylindrical shaped surface onto which the rim can be shrunk. After the horizontal keys have been adjusted, the degree of interference (shrink) is controlled by the insertion of a shrink shim between the rim and the key assembly.

The estimated / budget price of a full set of these keys is \$32,000.

b) Anti-buckling Stiffeners

With the high level of inward radial force that will be imposed onto the rotor spider arm blocks with the shrink, the analysis indicates that some plates of the rotor spider will buckle. To overcome this condition, angle shaped stiffeners must be welded to the top spider disk between arms (total of 8) and onto the arm web between the top and bottom disks (1 per arm – total of 8).

The budget price of these stiffeners is approximately \$1500.

